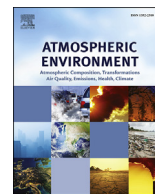




Contents lists available at ScienceDirect

Atmospheric Environment

journal homepage: www.elsevier.com/locate/atmosenv

Evaluating NO_x emission inventories for regulatory air quality modeling using satellite and air quality model data



Susan Kemball-Cook ^{a,*}, Greg Yarwood ^a, Jeremiah Johnson ^a, Bright Dornblaser ^b, Mark Estes ^b

^a ENVIRON International Corporation, 773 San Marin Drive, Suite 2115, Novato, CA, USA

^b Texas Commission on Environmental Quality, 12100 Park 35 Circle, MC 164, Austin, TX 78711, USA

HIGHLIGHTS

- We used OMI and CAMx NO₂ columns to estimate NO_x emissions over the southeast U.S.
- NO_x emissions estimates were developed using DOMINO v2.0 and NASA SP2 retrievals.
- The two top–down NO_x estimates were quite different over the southeast U.S.
- These disparities were due to differences in the two NO₂ retrievals.
- It was not possible to constrain the TCEQ's NO_x inventory with these estimates.

ARTICLE INFO

Article history:

Received 21 October 2014

Received in revised form

2 April 2015

Accepted 2 July 2015

Available online 10 July 2015

Keywords:

Satellite

NO_x

OMI

Model

Emissions

Ozone

ABSTRACT

The purpose of this study was to assess the accuracy of NO_x emissions in the Texas Commission on Environmental Quality's (TCEQ) State Implementation Plan (SIP) modeling inventories of the southeastern U.S. We used retrieved satellite tropospheric NO₂ columns from the Ozone Monitoring Instrument (OMI) together with NO₂ columns from the Comprehensive Air Quality Model with Extensions (CAMx) to make top–down NO_x emissions estimates using the mass balance method. Two different top–down NO_x emissions estimates were developed using the KNMI DOMINO v2.0 and NASA SP2 retrievals of OMI NO₂ columns. Differences in the top–down NO_x emissions estimates made with these two operational products derived from the same OMI radiance data were sufficiently large that they could not be used to constrain the TCEQ NO_x emissions in the southeast. The fact that the two available operational NO₂ column retrievals give such different top–down NO_x emissions results is important because these retrievals are increasingly being used to diagnose air quality problems and to inform efforts to solve them. These results reflect the fact that NO₂ column retrievals are a blend of measurements and modeled data and should be used with caution in analyses that will inform policy development. This study illustrates both benefits and challenges of using satellite NO₂ data for air quality management applications. Comparison with OMI NO₂ columns pointed the way toward improvements in the CAMx simulation of the upper troposphere, but further refinement of both regional air quality models and the NO₂ column retrievals is needed before the mass balance and other emission inversion methods can be used to successfully constrain NO_x emission inventories used in U.S. regulatory modeling.

© 2015 Elsevier Ltd. All rights reserved.

1. Introduction

Texas has two metropolitan areas, Houston–Galveston–Brazoria and Dallas–Fort Worth, which do not attain the National Ambient Air Quality Standard (NAAQS) for ozone. The Texas Commission on Environmental Quality (TCEQ) carries out ozone modeling as part of the Texas State Implementation Plan (SIP) that prescribes emissions controls that will allow these areas to attain the NAAQS in the

* Corresponding author.

E-mail addresses: skemballcook@enviromcorp.com (S. Kemball-Cook), gyarwood@enviromcorp.com (G. Yarwood), jjohnson@enviromcorp.com (J. Johnson), Bright.Dornblaser@tceq.texas.gov (B. Dornblaser), Mark.Estes@tceq.texas.gov (M. Estes).

future. Ozone transport has been shown to play an important role in determining ozone levels in Texas (Berlin et al., 2013). The southeastern U.S. sometimes is a source of ozone transport into Texas. A systematic high bias is present in the TCEQ's modeling of southeast ozone that can confound efforts to quantify the effects of ozone transport on Texas (ENVIRON, 2011). A high bias in modeled ozone in the southeast has been noted across multiple models (e.g. Herwehe et al., 2011; Chai et al., 2013). Model overestimates of ozone in the southeast may result, at least in part, from biased NOx emissions. The purpose of this study was to assess the accuracy of the NOx emissions data in the TCEQ's SIP modeling inventories, which are based on the 2005 National Emission Inventory (NEI) in the southeast.

Satellite NO₂ column retrievals have been used together with chemistry-transport models to provide constraints on global and regional NOx emission inventories by many investigators (e.g. Leue et al., 2001; Martin et al., 2003, 2006; Kononov et al., 2006; Zhang et al., 2007; Boersma et al., 2008; Napelenok et al., 2008; Kim et al., 2009; Lin et al., 2010; Miyazaki et al., 2012; Tang et al., 2013, 2014; Vinken et al., 2014). A review of methods is provided in Streets et al. (2013).

We evaluated the feasibility of using satellite NO₂ column data from the Ozone Monitoring Instrument (OMI) together with NO₂ columns from a regional air quality model to constrain the TCEQ's NOx emission inventory for the southeast. Following the mass balance method (Martin et al., 2003, 2006; Boersma et al., 2008; Lamsal et al., 2010; Tang et al., 2013), the ratio of the observed NO₂ columns to modeled NO₂ columns from the Comprehensive Air quality Model with extensions (CAMx; ENVIRON, 2014) was used together with the existing TCEQ bottom-up NOx emission inventory to estimate top-down NOx emissions. The top-down emission estimates are given by:

$$NOx\ Emiss_{top\ down} = \frac{\Omega_{satellite}}{\Omega_{model}} \times (NOx\ Emiss_{bottom\ up}) \times (Smoothing\ Factor) \quad (1)$$

where Ω are integrated tropospheric NO₂ vertical column densities (VCD; molecules cm⁻²) from the satellite retrieval and the air quality model. The smoothing factor accounts for the potential for NOx emissions to be transported out of a given grid cell and influence NO₂ columns beyond the grid cell in which emissions occurred.

In many previous studies, a single satellite retrieval was used to determine top-down NOx emissions constraints. In order to understand the uncertainty introduced into the top-down NOx emission estimates by the choice of retrieval, we used two independent operational retrievals to develop two different sets of top-down NOx emissions estimates. This is the first study we are aware of that compares top-down gridded regional emissions estimates developed using multiple satellite retrievals in order to assess method uncertainties.

The two sets of calculated top-down NOx emissions were compared with the TCEQ NOx emission inventory across the southeast. The comparison was carried out for May 31–July 2, 2006. This June 2006 episode is used by the TCEQ for regulatory ozone modeling.

2. Methods

2.1. Tropospheric NO₂ vertical column density data

2.1.1. OMI tropospheric NO₂ column retrieval

NO₂ column data are derived from measurements of

backscattered solar radiation made by OMI, a nadir-viewing UV–visible spectrometer (Levelt et al., 2006). OMI flies aboard NASA's Aura satellite, a polar orbiter that provides daily global coverage (Schoeberl et al., 2006; Boersma et al., 2007, 2011). Aura is in a sun-synchronous orbit with overpass at ~1:40 pm local time.

OMI does not measure NO₂ directly, but measures both direct sunlight and sunlight that is backscattered from the earth's atmosphere. Conversion of measured radiation from the OMI instrument to vertical tropospheric NO₂ columns is a multi-step process known as a retrieval. There is no unique solution for the vertical NO₂ column density given a set of measured OMI reflectances. The goal of the retrieval is to calculate the integrated vertical column of NO₂ that best reproduces the reflectances measured by OMI, given our knowledge of the characteristics of the instrument, the satellite viewing geometry and the relevant properties of the earth and the atmosphere.

2.1.2. DOMINO and SP2 retrievals

The first retrieval used in this study is the Derivation of OMI tropospheric NO₂ product (DOMINO; available from the Tropospheric Emission Monitoring Internet Service [TEMIS] at <http://www.temis.nl/>) product developed by KNMI (Koninkrijk Nederlands Meteorologisch Instituut). The DOMINO v2.0 OMI NO₂ column data product was the most recent version of the DOMINO product available at the time of this study (Boersma et al., 2011; Boersma and van der A, 2011). The second retrieval used here is version 2 of the NASA Standard Product (SP2; Bucsela et al., 2013). Although the two retrievals begin with the same slant NO₂ columns, they differ in some of their input data, their atmospheric mass factor calculations, and their stratospheric NO₂ column separation methods (Boersma et al., 2011; Bucsela et al., 2013) (See Supporting information for additional description of the retrieval process). There can be significant differences between the NO₂ columns produced by two different retrievals given the same OMI radiance data (Lamsal et al., 2010; Bucsela et al., 2008; Herron-Thorpe et al., 2010). It is not possible to say, based on available evaluations of the retrievals (e.g. Lamsal et al., 2014), whether one is more accurate than the other across the southeast during the June 2006 episode.

2.2. CAMx air quality model

CAMx was used to model the continental United States using nested 36/12/4 km resolution grids (See map in Supporting information). CAMx is a three-dimensional chemical-transport grid model and is used for ozone air-quality planning in Texas (TCEQ, 2010). The model was applied from the earth's surface upward to a height of approximately 15 km (vertical grid structure is shown in the Supporting information).

The June 2006 CAMx modeling databases were developed by the TCEQ for regulatory modeling of ozone. Meteorological input data for CAMx were developed using the Weather Research and Forecasting Model version 3.2 (WRF; Skamarock and Klemp, 2007). Boundary conditions for the outermost (36 km) grid were derived from a GEOS-Chem (Bey et al., 2001) global chemistry-transport model simulation of 2006. Emissions of VOCs, NOx, and CO from the TCEQ's 2006 emission inventory (TCEQ, 2010) were used. Throughout the modeling domain, emissions for U.S. power plants that report continuous emissions monitoring data to the U.S. EPA's Clean Air Markets Database were modeled at actual hourly June 2006 levels. For sources other than power plants, the TCEQ based the 2006 inventory on the 2005 NEI outside Texas and developed a detailed 2006 emission inventory based on local data for Texas. The Carbon Bond 6 chemical mechanism (CB6; Yarwood et al., 2010, 2012) was used.

The existing TCEQ SIP modeling June 2006 emission inventory was augmented with Fire Emission Inventory from NCAR (FINN) day-specific fire emissions derived from satellite observations (Wiedinmyer et al., 2011), Emissions Database for Global Atmospheric Research (EDGAR) aircraft emissions and lightning NO_x (LNO_x) emissions. LNO_x emissions were calculated using the parameterization of Koo et al. (2010). LNO_x emissions were allocated to grid cells where modeled convection occurred using convective precipitation as a proxy for lightning activity and were distributed in the vertical using the profiles of Ott et al. (2010). A description of both inventories is provided in the [Supporting information](#).

CAMx was run for the June 2006 episode, and a model performance evaluation for ozone, NO₂ and NO_x was carried out for monitoring sites in Texas and the southeast. The model performance evaluation showed that CAMx generally performed well in simulating ozone in urban areas of East Texas, but had an overall high bias (see [Supporting information](#); we refer to this simulation as the initial CAMx run).

2.3. Processing of retrieval data

We began with the NASA SP2 and DOMINO Level II datasets. Because the presence of clouds can cause significant bias in NO₂ columns (~60%; Boersma et al., 2004), we used only pixels with a cloud radiance fraction less than a threshold of 0.3 (Boersma et al., 2011). Pixels flagged as potentially containing artifacts due to ice, sun glint, eclipses, etc. were also discarded.

In order to compare the modeled CAMx NO₂ columns with the retrieved columns and use the mass balance method to prepare top–down emissions estimates, it is necessary to apply the OMI averaging kernel (AK) to the CAMx NO₂ VCD profiles before integrating the CAMx VCD through the depth of the troposphere to produce the final modeled VCD estimate (Rodgers, 2000; Eskes and Boersma, 2003; Boersma et al., 2011). The DOMINO v2.0 product provides the AK for each pixel. The NASA SP2 product provides scattering weights from which the AK can be calculated. We calculated AKs for the NASA SP2 retrieval for all pixels within the OMI swaths used for the June 2006 episode (see [Supporting information](#) for description of method). Next, we applied the AKs for each retrieval to the CAMx output to produce two sets of modeled VCD. The first was a set of CAMx modeled VCD to which the DOMINO AK had been applied; this set of columns was compared to the DOMINO retrieved columns. The second was a set of CAMx modeled VCD to which the SP2 AK had been applied; this set of columns was compared to the SP2 retrieved columns.

We compared the retrieved OMI tropospheric VCD with CAMx modeled VCD. Across the eastern U.S. and throughout the modeling episode, CAMx NO₂ columns were consistently lower than the OMI NO₂ columns from both retrievals (not shown). A low bias relative to OMI NO₂ columns has been noted for other regional air quality models (Huijnen et al., 2010; Allen et al., 2012). CAMx surface performance for NO₂ was evaluated against research-grade surface NO₂ measurements at SouthEastern Aerosol Research and Characterization (SEARCH; Hansen et al., 2003) monitoring sites in the southeast as well as against INTEX-A NO₂ measurements from the DC-8 aircraft (Singh et al., 2007) (see [Supporting information](#)). The evaluation showed that CAMx did not have a persistent low bias relative to SEARCH NO₂ measurements; this suggested that the surface NO_x emission inventory was not the cause for the CAMx NO₂ column low bias relative to OMI NO₂ columns. The model had a low bias for upper tropospheric NO₂, which we addressed through addition of downward transport of NO_y and ozone from the stratosphere, an updated aircraft emission inventory, a new version of the CB6 chemical mechanism (Yarwood et al., 2012), and

parameterized vertical transport of chemical species within clouds. The effects of each of these changes were evaluated separately and are discussed in the [Supporting information](#). The model updates that had the largest effect on the vertical profiles of NO_y in the upper troposphere and tropospheric NO₂ VCD were the addition of a stratospheric NO_y source and a more detailed aircraft emission inventory.

Following these changes, NO₂ performance in the upper troposphere improved, with the modeled NO₂ profile taking on the “C” shape seen in the observations, and a reduction in normalized bias near the tropopause from –66% to –23%. This improved agreement allowed the study to move forward, but does not demonstrate that the CAMx NO₂ columns are correct or that they show improved agreement with the retrieved VCD for the right reasons.

3. Results

3.1. Comparison of the DOMINO and SP2 episode average retrieved NO₂ VCD

Once the final model run had been completed, we recalculated the CAMx VCD and compared the modeled and retrieved columns ([Fig. 1](#)). The overall patterns of VCD are similar for the DOMINO and SP2 retrievals, with generally higher VCD over urban areas such as Chicago, Houston and the northeast corridor, and lower VCD over water and rural areas. The left panel of [Fig. 2](#) compares the DOMINO and SP2 episode average retrieved VCD for all grid cells. The retrievals are well-correlated ($r^2 = 0.81$), with the DOMINO retrieval showing larger VCD for grid cells with the highest VCD located in the New York and Chicago urban areas.

There are significant differences between the two retrievals, most notably over the southeast. [Fig. 1](#) shows that the SP2 retrieval has higher VCD over much of the southeast, including the Atlanta area, whose maximum is higher in SP2 than in DOMINO. The right hand panel of [Fig. 2](#) indicates that the two retrievals are reasonably well-correlated over the southeast ($r^2 = 0.55$) but the SP2 VCD are generally larger than the DOMINO VCD. The reason for this difference is not clear.

Comparison of the CAMx VCD following application of the SP2 and DOMINO AKs ([Fig. 1](#)) shows that the modeled VCD has similar patterns of high and low VCD to the retrieved VCD, with higher VCD over urban areas than in rural regions and higher VCD over the continent than offshore. [Fig. 3](#) compares the retrieved VCD with CAMx modeled VCD using DOMINO and SP2 AKs. The CAMx VCD is well-correlated with both retrievals ($r^2 = 0.77$ and 0.78 for DOMINO and SP2 retrievals, respectively) with better agreement for lower values of the retrieved VCD. Using both the DOMINO and SP2 AKs, CAMx has urban maxima that are more intense than in the retrievals (e.g. Houston, Atlanta, Chicago, Northeast corridor). This is likely because CAMx has higher spatial resolution than the models used to develop the retrievals and better resolves regions of high urban NO₂.

When the ratios (Retrieved VCD/CAMx VCD) are taken using the two retrievals (right panels of [Fig. 1](#)), striking differences emerge. In the southeast, the area of interest for the NO_x emission inventory assessment, the SP2/CAMx VCD ratio is generally >1 outside urban areas. Outside urban areas, the DOMINO/CAMx VCD ratio is generally close to 1 or <1 in the southeast. This difference in the retrieval/CAMx ratios occurs because the DOMINO VCD is lower than the SP2 retrieval throughout much the southeast ([Fig. 2](#), right panel), while the CAMx VCD is fairly similar in the southeast following application of the SP2 and DOMINO AKs. The differences noted above in the retrieval/CAMx VCD ratios directly affect top–down emissions estimates developed via the mass balance method.

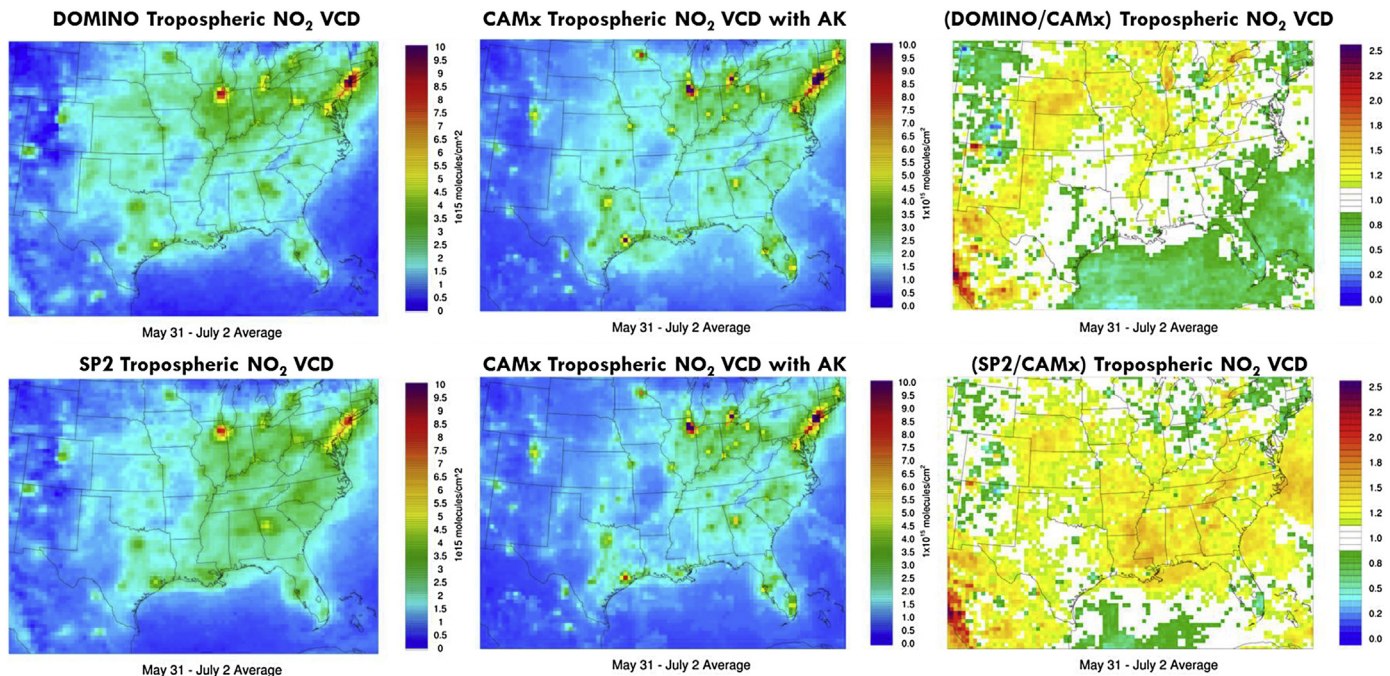


Fig. 1. Upper panels: (Left) DOMINO retrieved episode average tropospheric NO₂ VCD. (Middle) CAMx episode average tropospheric NO₂ VCD using DOMINO averaging kernel (AK). (Right) Ratio of DOMINO to CAMx episode average tropospheric NO₂ VCD. Lower panels: (Left) SP2 retrieved episode average tropospheric NO₂ VCD. (Middle) CAMx episode average tropospheric NO₂ VCD using SP2 AK. (Right) Ratio of SP2 to CAMx episode average tropospheric NO₂ VCD.

3.2. Top-down NO_x emission inventory estimates

We developed two separate top-down NO_x emission inventories using CAMx together with the DOMINO and SP2 retrievals. For the DOMINO case, the top-down emissions estimates were calculated for each grid cell using:

$$\begin{aligned}
 (\text{Top Down NO}_x \text{ Emissions})_{\text{DOMINO}} &= \left(\frac{\Omega_{\text{DOMINO}}}{\Omega_{\text{CAMx}}^{\text{DOMINO}}} \right) \\
 &\quad \times \text{TCEQ NO}_x \text{ Emissions} \\
 &\quad \times \text{Smoothing}
 \end{aligned}
 \quad (2)$$

$\Omega_{\text{CAMx}}^{\text{DOMINO}}$ is the CAMx column with the DOMINO AK applied to it. A second top-down emissions estimate was prepared using the NASA SP2 retrieval:

$$\begin{aligned}
 (\text{Top Down NO}_x \text{ Emissions})_{\text{SP2}} &= \left(\frac{\Omega_{\text{SP2}}}{\Omega_{\text{CAMx}}^{\text{SP2}}} \right) \times \text{TCEQ NO}_x \text{ Emissions} \\
 &\quad \times \text{Smoothing}
 \end{aligned}
 \quad (3)$$

$\Omega_{\text{CAMx}}^{\text{SP2}}$ is the CAMx column with the NASA SP2 AK applied to it. The two top-down emissions estimates derived using the SP2 and DOMINO retrievals were then compared to the augmented version

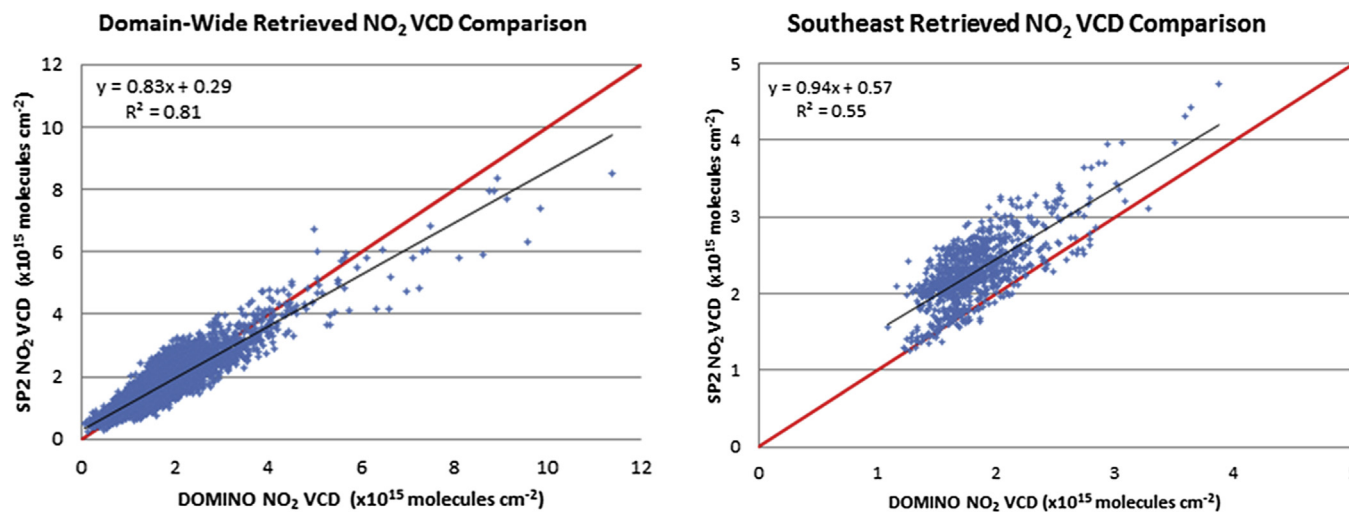


Fig. 2. Comparison of episode average retrieved tropospheric NO₂ VCD for entire domain shown in Fig. 1 (left) and southeast region consisting of Louisiana, Arkansas, Mississippi, Alabama, Georgia, Florida, South Carolina, and Tennessee (right). Red line is 1:1 line. Black line is linear best fit. (For interpretation of the references to colour in this figure legend, the reader is referred to the web version of this article.)

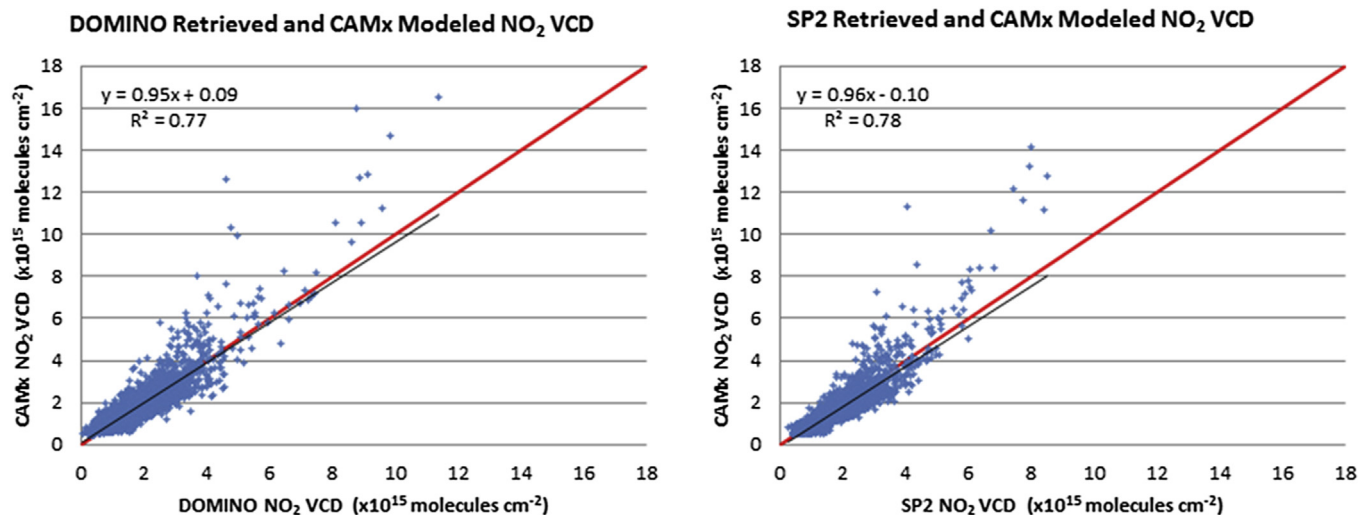


Fig. 3. Comparison of episode average retrieved and modeled tropospheric NO_2 VCD shown in Fig. 1. Left: DOMINO and CAMx VCD. Right: SP2 and CAMx VCD. Red line is 1:1 line. Black line is linear best fit. (For interpretation of the references to colour in this figure legend, the reader is referred to the web version of this article.)

of the TCEQ NO_x emission inventory that contains emissions from lightning, wildfires and aircraft.

The lifetime of NO_x over the U.S. in summer during OMI overpass hours is on the order of 7 h (Lamsal et al., 2010). For the 36 km grid cells in the TCEQ modeling domain, it is possible that the NO_2 column for a given grid cell may be influenced by NO_x emissions from neighboring grid cells. If a grid cell with large NO_x emissions lies adjacent to a cell with small NO_x emissions, the retrieved NO_2 column in the grid cell with small emissions may be affected by emissions in the cell with large emissions via transport. The top-down emissions estimate will therefore spuriously attribute emissions to the grid cell with small NO_x emissions. Others have identified this problem and compensated by spatially smoothing the emission inventories (Martin et al., 2003; Boersma et al., 2008; Tang et al., 2013).

As part of the emission inventory development, we investigated several different methods for spatial smoothing of the bottom-up emission inventory. Ideally, the smoothing would approximate the effect of advecting NO_x emissions from the grid cell in which they are emitted into surrounding cells. We determined that the spatial smoothing method that appears in the literature (e.g. Boersma et al., 2008; Tang et al., 2013) does not reproduce the expected characteristics of a NO_x emissions field smoothed by advection and gives top-down emission inventory results that contain numerical artifacts and are not useful in constraining the TCEQ's SIP modeling emission inventory. Therefore, the smoothing factor in equation (1) was set to 1 in the results that are presented here, although the lack of smoothing introduces error into the top-down emissions estimates through attribution of NO_2 to grid cells adjacent to sources of NO_x emissions. The magnitude of this error is dependent on the intensity of the NO_x emissions and the local wind field, and we discuss its effect on the results of this study below.

The TCEQ column-integrated episode average bottom-up NO_x emissions are shown in Fig. 4(a). The NO_x emissions show maxima coincident with large cities and major point sources such as the power plants in the Four Corners Area. Emissions from aircraft and ships are evident over the Gulf of Mexico and the Atlantic Ocean. Fig. 4(b) presents the difference between the top-down NO_x emission inventories produced using equations (2) and (3) and the bottom-up NO_x emission inventory shown in Fig. 4(a). The two lower panels of Fig. 4 show regions where the OMI data may

indicate biases in the TCEQ bottom-up inventory. There are regions where the top-down NO_x emission inventories are consistent in their difference from the bottom-up NO_x inventory, such as Dallas, Houston and Miami. Over the southeast, however, the two top-down inventories are not consistent in their differences from the bottom-up inventory. The top-down inventory developed using CAMx and the SP2 retrieval (EI_{SP2} ; lower right panel) has higher NO_x emissions than the TCEQ bottom-up inventory across broad areas of the southeast, while the top-down inventory developed using CAMx and the DOMINO retrieval ($\text{EI}_{\text{DOMINO}}$) is either generally comparable to (Mississippi, Louisiana, Alabama, Georgia) or is lower than (North and South Carolina) the bottom-up inventory.

Fig. 5 compares the two top-down emission inventories over the southeast. The two inventories are very well-correlated ($r^2 = 0.99$), as expected given that they are both based on the same CAMx simulation and bottom-up inventory, but EI_{SP2} is consistently higher than $\text{EI}_{\text{DOMINO}}$.

It is not known which top-down inventory is more accurate, so it is not possible to determine whether there is a systematic bias in the bottom-up NO_x emission inventory based on these results.

As noted above, the top-down emission inventories were calculated without spatial smoothing. The inventories are influenced only by the ratio of modeled columns to satellite columns, and may contain error due to attribution of emissions into grid cells near NO_x sources due to advection of NO_x out of the grid cells into which they were emitted. Previous studies have employed spatial smoothing to approximate the advection of NO_x emissions from the grid cell in which they are emitted into surrounding cells. Our analysis was for a month-long period over which time local wind fields varied substantially in response to many factors. Rather than attempting to use smoothing factors to describe effects of varying wind fields, we took a different approach of integrating comparisons over geographic areas (states) that are sufficiently large as to encompass urban areas that could require smoothing. Integrating over states has the advantage of comparability with emission inventories. We performed a state-level comparison of the VCD and top-down and bottom-up inventories to minimize the effect of the attribution error described above. The method and results are described in the Supporting information, and the results are consistent with those shown in Figs. 1–5. We conclude that this attribution error does not significantly affect our emission inventory results over the southeast.

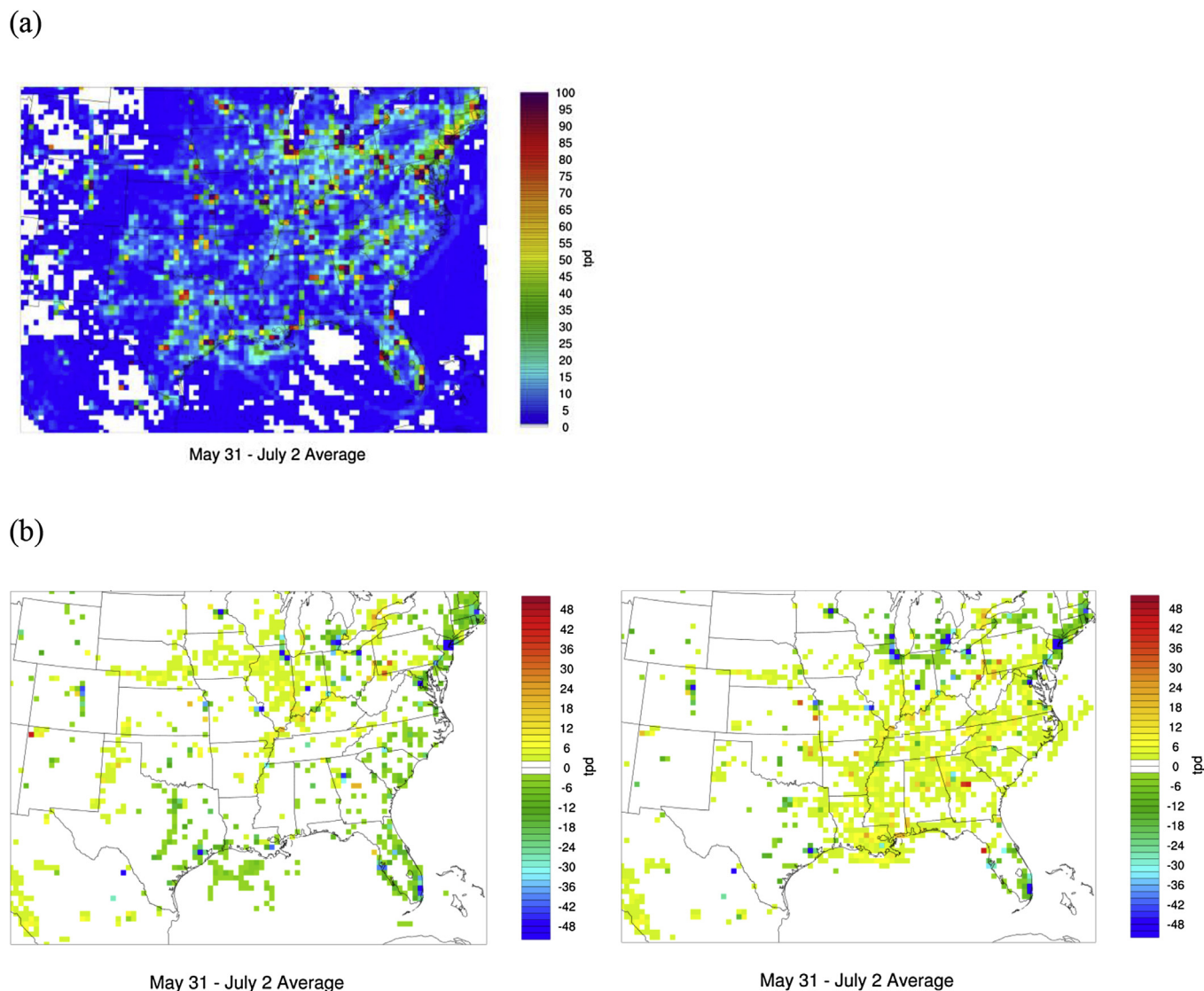


Fig. 4. (a): Episode average emissions for the TCEQ June 2006 episode NO_x emission inventory (bottom–up NO_x emission inventory). (b): Top–down NO_x emission inventory – bottom–up NO_x emission inventory using CAMx with DOMINO (lower left panel) and SP2 (lower right panel) retrievals. No smoothing was performed in the calculation of these emissions estimates. Emissions estimates are in tons per day (tpd).

4. Discussion

We evaluated the feasibility of using DOMINO and SP2 tropospheric NO₂ column retrievals together with CAMx NO₂ columns to make two top–down NO_x emissions estimates for the southeast to constrain the TCEQ's SIP modeling NO_x emission inventories. The two sets of NO_x emissions estimates were found to have significant differences over the southeast. These differences were large enough to confound efforts to gain information from the top–down estimates that could constrain the TCEQ inventory and stemmed from differences in the SP2 and DOMINO retrieved VCD over the southeast.

The fact that the two available operational NO₂ column retrievals give such different top–down NO_x emissions results is important because these retrievals are increasingly being used to diagnose air quality problems and to inform efforts to solve them. Determining the factor(s) that cause differences between retrievals is an area for future research and refinement of the retrievals.

This study points out the dependence of top–down emission

inventory results on the choice of retrieval. A technique that is becoming more prevalent in the application of the mass balance method is to use the air quality model's NO₂ profile to calculate a new atmospheric mass factor, essentially developing a new retrieval which has as its *a priori* NO₂ profile the modeled NO₂ profile shape (e.g. Lamsal et al., 2010; Tang et al., 2014; Vinken et al., 2014). Lamsal et al. (2010) note that this method allows a more consistent comparison with the air quality model. The utility of developing such a retrieval depends on confidence in the NO_x emission inventory and the model's simulation of NO₂ and its reservoir species. This study points out the dependence of the retrievals on the assumptions that go into them and reflects the fact that they are a blend of measurements and modeled data and should be used with caution in analyses that will inform policy development.

This study also shows how satellite data used together with aircraft measurements can be a powerful tool for evaluating and improving air quality models. Underestimates of retrieved VCD in CAMx noted in the comparison of the initial CAMx modeled NO₂

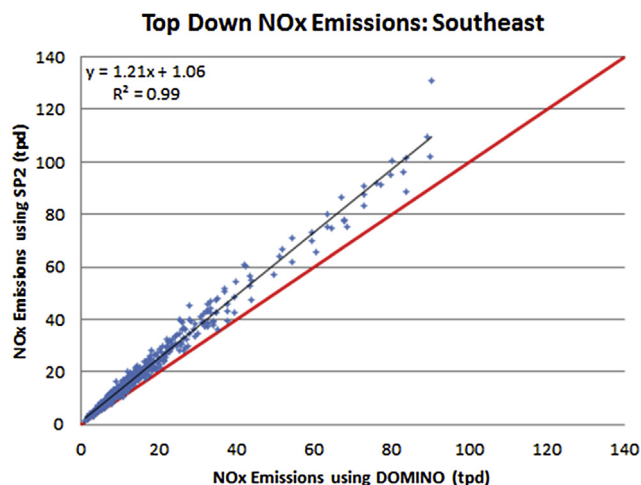


Fig. 5. Comparison of top-down NO_x emissions calculated using CAMx together with DOMINO and SP2 retrievals for southeast region consisting of Louisiana, Arkansas, Mississippi, Alabama, Georgia, Florida, South Carolina, and Tennessee. Red line is 1:1 line. Black line is linear best fit. (For interpretation of the references to colour in this figure legend, the reader is referred to the web version of this article.)

columns with retrieved columns led to the first evaluation of CAMx against aircraft observations of the upper troposphere. This comparison showed that, like other regional and global models, CAMx underestimated NO₂, NO_x, and NO_y in the upper troposphere. Once this bias had been identified, we were able to take steps to reduce it, allowing the model to be used in further comparisons with satellite NO₂ VCD retrievals.

The addition of transport of NO_y from the stratosphere to the troposphere was the model update that had the largest effect on the upper tropospheric NO₂ and VCD, and spurred development of CAMx capability to read in a spatially/temporally varying top concentration obtained from a global model simulation. This allows for an improved simulation of cross-tropopause transport and upper tropospheric NO_y. Another need identified was for CAMx to include a simulation of vertical transport of chemical species by deep convection. Given the importance of convection in venting polluted air from the surface layer and transporting chemical species to the free troposphere, it is critical that a physically-based parameterization of convective transport of chemical species be integrated into CAMx. This work is underway. With these important components of the simulation of the upper troposphere in place, the CAMx model will be better able to simulate NO₂ columns required for top-down emissions estimation. Models that do not contain an accurate simulation of processes affecting the upper troposphere, such as cross-tropopause transport and a detailed characterization of aircraft cruise emissions, should not be used for emissions evaluation using column-integrated satellite products.

Acknowledgments

We acknowledge the free use of tropospheric NO₂ column data from the OMI sensor from www.temis.nl as well as the use of the NASA SP2 retrieval. We wish to thank the University of Wisconsin–Madison for the use of the Wisconsin Horizontal Interpolation Program for Satellites (WHIPS). WHIPS was developed by Jacob Oberman, Erica Scotty, Keith Maki and Tracey Holloway, with funding from the NASA Air Quality Applied Science Team (AQAST) and the Wisconsin Space Grant Consortium Undergraduate Award. We thank Barron Henderson for providing the INTEX-A NASA DC-8 flight dataset and for helpful discussions. This work was sponsored by the Texas Commission on Environmental Quality.

Appendix A. Supplementary data

Supplementary data related to this article can be found at <http://dx.doi.org/10.1016/j.atmosenv.2015.07.002>.

References

- Allen, D.J., Pickering, K.E., Pinder, R.W., Henderson, B.H., Appel, K.W., Prados, A., 2012. Impact of lightning-NO on Eastern United States photochemistry during the summer of 2006 as determined using the CMAQ model. *Atmos. Chem. Phys.* 12, 1737–1758. <http://dx.doi.org/10.5194/acp-12-1737-2012>.
- Berlin, S., Langford, A.O., Estes, M., Dong, M., Parrish, D.D., 2013. Magnitude, decadal changes, and impact of regional background ozone transported into the Greater Houston, Texas, area. *Env. Sci. Tech.* 47, 13,985–13,992. <http://dx.doi.org/10.1021/es4037644>.
- Bey, I., Jacob, D.J., Yantosca, R.M., Logan, J.A., Field, B.D., Fiore, A.M., Li, Q., Liu, H.Y., Mickley, L.J., Schultz, M.G., 2001. Global modeling of tropospheric chemistry with assimilated meteorology: model description and evaluation. *J. Geophys. Res.* 106 (D19), 23073–23095. <http://dx.doi.org/10.1029/2001JD000807>.
- Boersma, K.F., Eskes, H.J., Brinkma, E.J., 2004. Error analysis for tropospheric NO₂ retrieval from space. *J. Geophys. Res.* 109, D04311.
- Boersma, K.F., Eskes, H.J., Veeckind, J.P., Brinkma, E.J., van der A, R.J., Sneep, M., van den Oord, G.H.J., Levelt, P.F., Stammes, P., Gleason, J.F., Bucsela, E.J., 2007. Near-real time retrieval of tropospheric NO₂ from OMI. *Atmos. Chem. Phys.* 7, 2103–2118. <http://dx.doi.org/10.5194/acp-7-2103-2007>.
- Boersma, K.F., Jacob, D.J., Bucsela, E.J., Perring, A.E., Dirksen, R., van der A, R.J., Yantosca, R.M., Park, R.J., Wenig, M.O., Bertram, T.H., Cohen, R.C., 2008. Validation of OMI tropospheric NO₂ observations during INTEX-B and application to constrain NO_x emissions over the eastern United States and Mexico. *Atmos. Environ.* 42 (19), 4480–4497. <http://dx.doi.org/10.1016/j.atmosenv.2008.02.004>.
- Boersma, K.F., Eskes, H.J., Dirksen, R.J., van der A, R.J., Veeckind, J.P., et al., 2011. An improved tropospheric NO₂ column retrieval algorithm for the ozone monitoring instrument. *Atmos. Meas. Tech.* 4, 1905–1928. <http://dx.doi.org/10.5194/amt-4-1905-2011>.
- Boersma, R., Braak, van der A, R.J., 2011. Dutch OMI NO₂ (DOMINO) Data Product v2.0 HE5 Data File User Manual. http://www.temis.nl/docs/OMI_NO2_HE5_2.0_2011.pdf.
- Bucsela, E.J., Perring, A.E., Cohen, R.C., Boersma, K.F., Celarier, E.A., Gleason, J.F., Wenig, M.O., Bertram, T.H., Wooldridge, P.J., Dirksen, R., Veeckind, J.P., 2008. Comparison of tropospheric NO₂ from in-situ aircraft measurements with near-real time and standard product data from OMI. *J. Geophys. Res.* 113, D16S31. <http://dx.doi.org/10.1029/2007JD008838>.
- Bucsela, E.J., Krotkov, N.A., Celarier, E.A., Lamsal, L.N., Swartz, W.H., Bhartia, P.K., Boersma, K.F., Veeckind, J.P., Gleason, J.F., Pickering, K.E., 2013. A new stratospheric and tropospheric NO₂ retrieval algorithm for nadir-viewing satellite instruments: applications to OMI. *Atmos. Meas. Tech. Discuss.* 6, 1361–1407.
- Chai, T., Kim, H.-C., Lee, P., Tong, D., Pan, L., Tang, Y., Huang, J., McQueen, J., Tsidulko, M., Stajner, I., 2013. Evaluation of the United States National Air Quality Forecast Capability experimental real-time predictions in 2010 using air quality system ozone and NO₂ measurements. *Geosci. Model Dev.* 6, 1831–1850. <http://dx.doi.org/10.5194/gmd-6-1831-2013>.
- ENVIRON, July 2011. Analysis of Ozone Contributions from Different Source Regions: Work Order No. 582-11-10396-FY11-01. Prepared for: Jocelyn Mellberg, Fernando Mercado and Mark Estes, TCEQ, 12100 Park 35 Circle Austin, TX. https://www.dropbox.com/s/6um01gaexnhg39f/WO_582-11-10396-FY11-01_final_report_072911.pdf.
- ENVIRON, October 2014. User's Guide to the Comprehensive Air Quality Model with Extensions Version 5.40. ENVIRON International Corporation, Novato, CA. Available at: www.camx.com.
- Eskes, H.J., Boersma, K.F., 2003. Averaging kernels for DOAS total column satellite retrievals. *Atmos. Chem. Phys.* 3, 1285–1291. <http://dx.doi.org/10.5194/acp-3-1285-2003>.
- Hansen, D.A., Edgerton, E.S., Hartsell, B.E., Jansen, J.J., Kandasamy, N., Hidy, G.M., Blanchard, C.L., 2003. The Southeastern aerosol research and characterization study. Part 1: overview. *J. Air Waste Manage. Assoc.* 53, 1460–1471. <http://dx.doi.org/10.1080/10473289.2003.10466318>.
- Herron-Thorpe, F.L., Lamb, B.K., Mount, G.H., Vaughan, J.K., 2010. Evaluation of a regional air quality forecast model for tropospheric NO₂ columns using the OMI/Aura satellite tropospheric NO₂ product. *Atmos. Chem. Phys.* 10, 8839–8854. <http://dx.doi.org/10.5194/acp-10-8839-2010>.
- Herwehe, J.A., Otte, T., Mathur, R., Rao, S., 2011. Diagnostic analysis of ozone concentrations simulated by two regional-scale air quality models. *Atmos. Environ.* 45, 5957–5969.
- Huijnen, V., Eskes, H.J., Amstrup, B., Bergstrom, R., Boersma, K.F., Elbern, H., Flemming, J., Foret, G., Friese, E., Gross, A., D'Isidoro, M., Kioutsioukis, I., Maurizi, A., Melas, D., Peuch, V.-H., Poupkou, A., Robertson, L., Sofiev, M., Stein, O., Strunk, A., Valdebenito, A., Zerefos, C., Zyryanov, D., 2010. Comparison of OMI NO₂ tropospheric columns with an ensemble of global and European regional air quality models. *Atmos. Chem. Phys.* 10, 3273–3296. <http://dx.doi.org/10.5194/acpd-9-22271-2009>.
- Kim, S.W., Heckel, A., Frost, G.J., Richter, A., Gleason, J., Burrows, J.P., McKeen, S., Hsie, E.Y., Granier, C., Trainer, M., 2009. NO₂ columns in the western United States observed from space and simulated by a regional chemistry model and

- their implications for NO_x emissions. *J. Geophys. Res.* 114, D11301. <http://dx.doi.org/10.1029/2008JD011343>.
- Kononov, I.B., Beekmann, M., Richter, A., Burrows, J.P., 2006. Inverse modeling of the spatial distribution of NO_x emissions on a continental scale using satellite data. *Atmos. Chem. Phys.* 6, 1747–1770. <http://dx.doi.org/10.5194/acp-6-1747-2006>.
- Koo, B., Chien, C.-J., Tonnesen, G., Morris, R., Johnson, J., Sakulyanontvittaya, T., Piyachaturawat, P., Yarwood, G., 2010. Natural emissions for regional modeling of background ozone and particulate matter and impacts on emissions control strategies. *Atmos. Environ.* 44, 2372–2382. <http://dx.doi.org/10.1016/j.atmosenv.2010.02.041>.
- Lamsal, L.N., Martin, R.V., van Donkelaar, A., Celarier, E.A., Bucsela, E.J., Boersma, K.F., Dirksen, R., Luo, C., Wang, Y., 2010. Indirect validation of tropospheric nitrogen dioxide retrieved from the OMI satellite instrument: insight into the seasonal variation of nitrogen oxides at northern midlatitudes. *J. Geophys. Res.* 115, D0530. <http://dx.doi.org/10.1029/2009JD013351>.
- Lamsal, L.N., Krotkov, N.A., Celarier, E.A., Swartz, W.A., Pickering, K.E., Bucsela, E.J., Martin, R.V., Philip, S., Irie, H., Cede, A., Herman, J., Weinheimer, A., Szykman, J.J., Knepp, T.N., 2014. Evaluation of OMI operational standard NO₂ retrievals using in situ and surface-based NO₂ observations. *Atmos. Phys. Chem. Discuss.* 14, 14519–14573.
- Leue, C., Wenig, M., Wagner, T., Klimm, O., Platt, U., Jahne, B., 2001. Quantitative analysis of NO_x emissions from global ozone monitoring experiment satellite image sequences. *J. Geophys. Res.* 106, 5493–5505.
- Levelt, P.F., Hilsenrath, E., Leppelmeier, G.W., van den Oord, G.B.J., Bhartia, P.K., Tamminen, J., de Haan, J.F., Veefkind, J.P., 2006. Science objectives of the ozone monitoring instrument. *IEEE Trans. Geosci. Remote Sens.* 44, 1199–1208. <http://dx.doi.org/10.1109/TGRS.2006.872333>.
- Lin, J.-T., McElroy, M.B., Boersma, K.F., 2010. Constraint of anthropogenic NO_x emissions in China from different sectors: a new methodology using multiple satellite retrievals. *Atmos. Chem. Phys.* 10, 63–78. <http://dx.doi.org/10.5194/acp-10-63-2010>.
- Martin, R.V., Jacob, D.J., Chance, K., Kurosu, T.P., Perner, P.I., Evans, M.J., 2003. Global inventory of nitrogen oxide emission constrained by space-based observations of NO₂ columns. *J. Geophys. Res.* 108 (D17), 4537. <http://dx.doi.org/10.1029/2003JD003453>.
- Martin, R.V., Sioris, C.E., Chance, K., Ryerson, T.B., Bertram, T.H., Wooldridge, P.J., Cohen, R.C., Neuman, J.A., Swanson, A., Flocke, F.M., 2006. Evaluation of space-based constraints on global nitrogen oxide emissions with regional aircraft measurements over and downwind of eastern North America. *J. Geophys. Res.* 111, D15308. <http://dx.doi.org/10.1029/2005JD006680>.
- Miyazaki, K., Eskes, H.J., Sudo, K., 2012. Global NO_x emission estimates derived from an assimilation of OMI tropospheric NO₂ columns. *Atmos. Chem. Phys.* 12, 2263–2288. <http://dx.doi.org/10.5194/acp-12-2263-2012>.
- Napelenok, S.L., Pinder, R.W., Gilliland, A.B., Martin, R.V., 2008. A method for evaluating spatially-resolved NO_x emissions using Kalman filter inversion, direct sensitivities, and space-based NO₂ observations. *Atmos. Chem. Phys.* 8, 5603–5614. <http://dx.doi.org/10.5194/acp-8-5603-2008>.
- Ott, L.E., Pickering, K.E., Stenchikov, G.L., Allen, D.J., DeCaria, A.J., Ridley, B., Lin, R.-F., Lang, S., Tao, W.-K., 2010. Production of lightning NO_x and its vertical distribution calculated from three-dimensional cloud-scale chemical transport model simulations. *J. Geophys. Res.* 115 (D4) <http://dx.doi.org/10.1029/2009JD011880>.
- Rodgers, C., 2000. *Inverse Methods for Atmospheric Sounding: Theory and Practice*. World Scientific, Singapore.
- Schoeberl, M.R., Douglass, A.R., Hilsenrath, E., Bhartia, P.K., Beer, R., Waters, J.W., Gunson, M., Froidevaux, L., Gille, J., Barnett, J., Levelt, P.F., Decola, P., 2006. Overview of the EOS aura mission. *IEEE Trans. Geosci. Remote Sens.* 44, 1066–1074.
- Singh, H.B., Salas, L., Herlth, D., Kolyer, R., Czech, E., Avery, M., Crawford, J.H., Pierce, R.B., Sachse, G.W., Blake, D.R., Cohen, R.C., Bertram, T.H., Perring, A., Wooldridge, P.J., Dibb, J., Huey, G., Hudman, R.C., Turquety, S., Emmons, L.K., Flocke, F., Tang, Y., Carmichael, G.R., Horowitz, L.W., 2007. Reactive nitrogen distribution and partitioning in the North American troposphere and lowermost stratosphere. *J. Geophys. Res.* 112 (D12S04) <http://dx.doi.org/10.1029/2006JD007664>.
- Skamarock, W.C., Klemp, J.B., 2007. A time-split nonhydrostatic atmospheric model for research and NWP applications. *J. Comp. Phys.* 3465–3485.
- Streets, D.G., Canty, T., Carmichael, G.R., de Foy, B., Dickerson, R.R., Duncan, B.N., Edwards, D.P., Haynes, J.A., Henze, D.K., Houyoux, M.R., Jacob, D.J., Krotkov, N.A., Lamsal, L.N., Liu, Y., Lu, Z., Martin, R.V., Pfister, G.G., Pinder, R.W., Salawitch, R.J., Wecht, K.J., 2013. Emissions estimation from satellite retrievals: a review of current capability. *Atmos. Environ.* 77, 1011–1042.
- Tang, W., Cohan, D., Lamsal, L.N., Xiao, X., Zhou, W., 2013. Inverse modeling of Texas NO_x emissions using space-based and ground-based NO₂ observations. *Atmos. Chem. Phys.* 13, 11005–11018. <http://dx.doi.org/10.5194/acp-13-11005-2013>.
- Tang, W., Cohan, D.S., Pour-Biazar, A., Lamsal, L.N., White, A., Xiao, X., Zhou, W., Henderson, B.H., Lash, B., 2014. Influence of satellite-derived photolysis rates and NO_x emissions on Texas ozone modeling. *Atmos. Chem. Phys. Discuss.* 14, 24475–24522. <http://dx.doi.org/10.5194/acpd-14-24475-2014>.
- Texas Commission on Environmental Quality, 2010. Houston-Galveston-Brazoria Attainment Demonstration State Implementation Plan Revision for the 1997 Eight-hour Ozone Standard. Project Number 2009-017-SIP-NR; Austin, TX. http://www.tceq.texas.gov/airquality/sip/HGB_eight_hour.html.
- Vinken, G.C.M., Boersma, K.F., van Donkelaar, A., Zhang, L., 2014. Constraints on ship NO_x emissions in Europe using GEOS-Chem and OMI satellite NO₂ observations. *Atmos. Chem. Phys.* 14, 1353–1369. <http://dx.doi.org/10.5194/acp-14-1353-2014>.
- Wiedinmyer, C., Akagi, S.K., Yokelson, R.J., Emmons, L.K., Al-Saadi, J.A., Orlando, J.J., Soja, A.J., 2011. The Fire INventory from NCAR (FINN): a high resolution global model to estimate the emissions from open burning. *Geosci. Model Dev.* 4 (3), 625–641.
- Yarwood, G., Jung, J., Whitten, G.Z., Heo, G., Mellberg, J., Estes, E., 2010. Updates to the Carbon Bond Mechanism for Version 6 (CB6). Presented at the 9th Annual CMAS Conference, Chapel Hill, October.
- Yarwood, G., Heo, G., Carter, W., Whitten, G., 2012. Final Report, Environmental Chamber Experiments to Evaluate NO_x Sinks and Recycling in Atmospheric Chemical Mechanisms. AQRP Project 10–042. Prepared for Dr. Elena C. McDonald-Buller, Texas Air Quality Research Program. <http://aqrp.ceer.utexas.edu/projectinfo%5C10-042%5C10-042%20Final%20Report.pdf>.
- Zhang, Q., Streets, D.G., He, K.B., Wang, Y.X., Richter, A., Burrows, J.P., Uno, I., Jang, C.J., Chen, D., Yao, Z.L., Lei, Y., 2007. NO_x emission trends for China, 1995–2004: the view from the ground and the view from space. *J. Geophys. Res.* 112, D22306. <http://dx.doi.org/10.1029/2007JD008684>.